

STABLE, HIGH-Q FABRY-PEROT RESONATORS WITH LONG CAVITY BASED ON CURVED, ALL-SILICON, HIGH REFLECTANCE MIRRORS

M. Malak¹, N. Pavy¹, F. Marty¹, Y.-A. Peter², A.Q. Liu³ and T. Bourouina¹

¹Université Paris-Est, laboratoire ESYCOM, ESIEE-Paris, Noisy-le-Grand, France

²Ecole Polytechnique de Montréal, Montréal, Québec, Canada

³Nanyang Technological University, Singapore, Singapore

ABSTRACT

For the first time, we demonstrate experimentally high optical quality factor $Q \sim 9000$ in MEMS-compatible silicon Fabry-Pérot (FP) resonators based on free space propagation of light and direct coupling to optical fiber. This result is obtained on long cavity resonators ($L > 250 \mu\text{m}$), a usually difficult case in terms of power loss. The resonator design includes two multilayered silicon-air Bragg mirrors of cylindrical shape, combined with a Fiber Rod Lens (FRL). Dimensions are chosen according to stability criteria imposed on the optical resonator. The core of the presented device is entirely made of single-crystal silicon. It is obtained by DRIE using an optimized single step process.

INTRODUCTION

Since its invention, the FP resonator became an important block in various optical applications. The first versions were bulky and expensive and were mainly used in the calibration of several equipments, taking advantage of their high performance. With the development of the micro-fabrication technologies, miniaturized versions of the free space FP resonator could be produced on silicon or SOI wafers. Design improvements have been introduced as well, so that the miniaturized devices gained a competing performance with respect to the early devices. Nowadays, as they are obtainable in batch processing using cheap materials, they acquired back special interest in many areas.

With particular attention to long air cavity resonators, our ultimate goal is to introduce significant improvement to the magical FP resonator that is being integrated in many applications: WDM filters [1], tunable laser sources [2], refractometry [3], as well as displacement measurement and biochemical sensing techniques. Indeed, in most of those applications, the system performance was found to be mainly dependent on the Q -factor of the FP response, which is the point addressed here.

At least five groups already reported on FP resonator based on *planar* silicon-air Bragg mirrors fabricated either by DRIE [1, 3, 4, 5] or by KOH etching [6]. In all cases, the cavity length was in the order of $10 \mu\text{m}$ only, mainly for the purpose of reducing the dominant loss mechanism, which relates to Gaussian beam expansion inside the cavity after several round trips. Nevertheless, these planar FP cavities are considered as “unstable resonators” [7] with Q -factor mostly limited to a few hundreds, except in [5] where silicon rib-waveguide was introduced leading to $Q=4200$.

DESIGN DESCRIPTION

In order to overcome the limited performance of conventional planar FP resonator, we introduce a novel FP architecture, in which we provide two major design improvements: The first improvement takes advantage of the novel cylindrical Bragg mirrors that act as concave mirrors along one transverse direction, (in-plane). So, they focus the light beam, which is not the case when using planar mirrors. The second improvement concerns the FRL that has been introduced inside the cavity gap to focus the Gaussian beam in the other transverse direction (out-of-plane). This combination provides a complete focusing solution, leading to light confinement inside the cavity. Photos of the fabricated device are shown in Figure 1 and 2.

The fabricated devices share common parameters. Every silicon layer has a width of $3.67 \mu\text{m}$, while the air layer has a width of $3.49 \mu\text{m}$. A long recess opening ($\sim 1 \text{ cm}$) of $128 \mu\text{m}$ width is shared between all the devices to facilitate the insertion of the FRL, whose width is $125 \mu\text{m}$. On the contrary, the fabricated FP cavities differ from each other, either in their physical length of the cavity or in the number of Bragg layers per mirror. Based on these settings, many combinations were generated, measured and then analyzed.

It is noteworthy that due to the added FRL inside the air cavity, the well-known stability conditions related to homogeneous cavities [7] no longer apply here. So, a dedicated mathematical model has been developed to study the stability limits and it will be outlined in the next section.

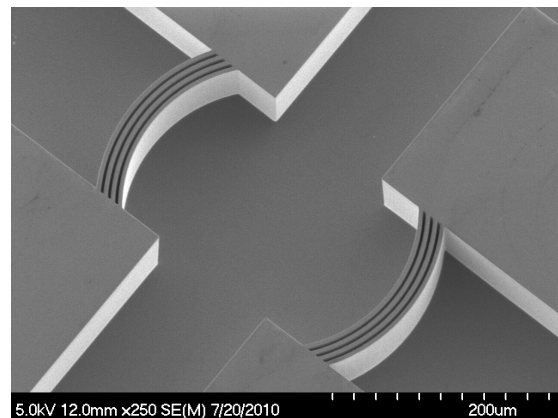


Figure 1: SEM photos of FP cavity with Bragg mirrors of cylindrical shape (Here 4 silicon-air layers with the DRIE trench for the Fiber Rod Lens (FRL))

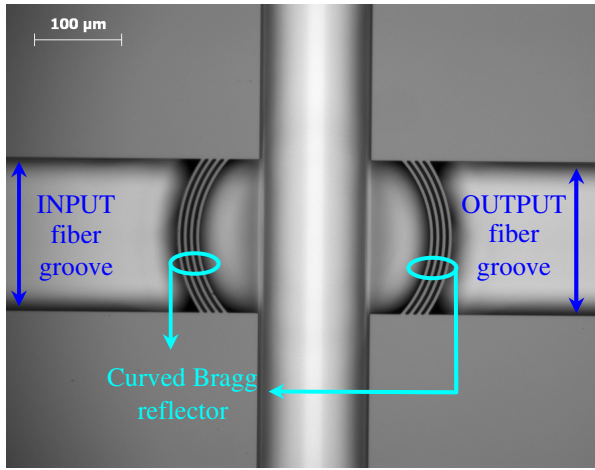


Figure 2: Microscopic photo of similar cavity as in Figure 1 but with Fiber Rod Lens (FRL) placed inside the DRIE recess for the purpose of ‘vertical’ out-of-plane collimation.

DESIGN FOR STABILITY

In order to determine the geometrical parameters of the newly designed cavities, such as the radius of curvature, R , and the free space propagation distances d and d_{fs} , we need to calculate the conditions of stability. To do so, optical resonators are usually modeled using the matrix approach [7]. In this approach, each ray is defined by a position “ y ” and angle “ θ ” with respect to the optical axis. These variables (y, θ) vary as the ray propagates along the optical system and they are related to the subsequent set of variables by a 2x2 transfer matrix. This is written in the following form:

$$\begin{pmatrix} y_2 \\ \theta_2 \end{pmatrix} = \begin{pmatrix} A & B \\ C & D \end{pmatrix} \begin{pmatrix} y_1 \\ \theta_1 \end{pmatrix} = K \begin{pmatrix} y_1 \\ \theta_1 \end{pmatrix} \quad (1)$$

where K is a 2x2 ray transfer, which represents each optical component. Consequently, the equivalent matrix of the whole system will be given by:

$$K_{eq} = K_n \dots K_2 K_1 \quad (2)$$

where K_{eq} is the system equivalent matrix and K_i is the matrix of the i^{th} component. Notice the order of multiplication is from the last element to the first one.

Now, we come back to the study of our optical resonator. It is the case of cascaded K_{eq} identical matrices [7]. This time, K_{eq} denotes the ray transfer matrix after one full round trip in the resonator, which means that m round trips of light can be modeled by the matrix $K_{tot} = K_{eq}^m$. After mathematical manipulations, the stability condition of the resonator is found to be given by:

$$\left| \frac{A' + D'}{2} \right| \leq 1 \quad (3)$$

Here, A' and D' denote the first and the fourth element of the full round trip matrix K_{eq} . Starting from this general result, and in order to derive the full conditions of stability, we need to apply it in two situations, corresponding to

different ways of seeing the system transversely.

First, when considering the system seen in the XZ cross-section, as schematized in Figure 3a, the propagating beam faces the following transformations (modeled through the corresponding transfer matrices):

1. Reflection from a concave mirror.
2. Free space propagation of distance d_x .
3. Refraction from air to fiber.
4. Propagation inside the fiber of distance d_f .
5. Refraction from fiber to air.

We assume that the multilayer Bragg mirror is simply a single interface having a high reflectance \mathfrak{R} . Also, we consider that the refractive index distribution of the fiber is uniform so we do not discriminate between the core and the cladding. After mathematical manipulations [8], we obtain first K_{eq} and then, applying the condition of stability mentioned in equation (3), we get:

$$0 \leq \frac{(2d_x + d_f/n_f)}{2|R|} \leq 1 \quad (4)$$

Secondly, we analyze the stability of the system seen in the YZ cross section, as schematized in Figure 3b. In this case, the following transformations apply:

1. Reflection from a straight mirror.
2. Free space propagation region.

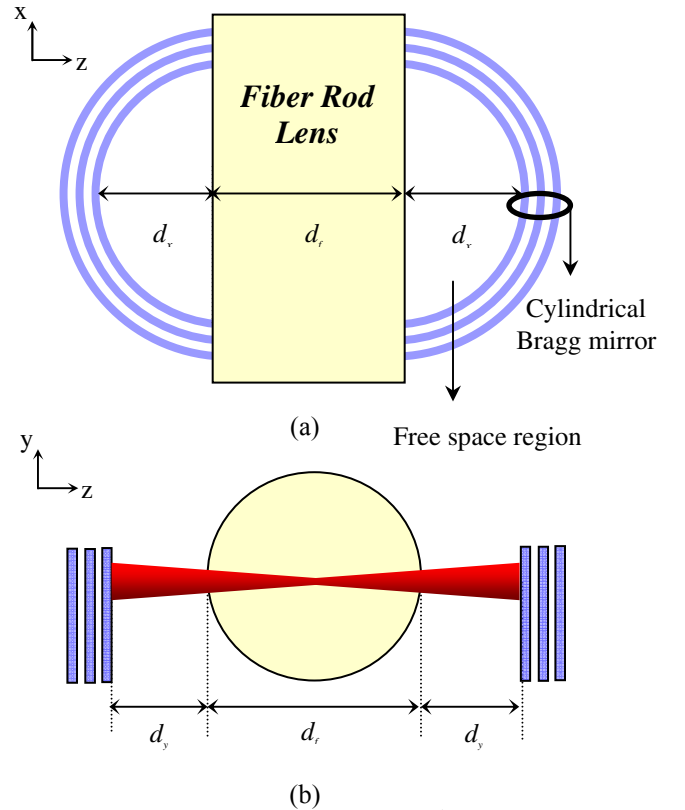


Figure 3: (a) Cross section view of the 2nd design in the XZ transverse plane (b) Cross section view of the same design in the YZ transverse plane. The functions of in-plane and out-of-plane focusing are described, respectively.

3. Refraction from air to curved fiber interface.
4. Propagation inside the fiber.
5. Refraction from curved fiber interface to air.

After tedious mathematical manipulations, we obtain K_{eq} . Then, applying again the condition of stability (3), we finally get the second stability condition as follow:

$$0 \leq (1 - 2/n_f) + (4d_y/d_f)(1 - 1/n_f) \leq 1 \quad (5)$$

By solving (4) and (5) for d_x and d_y , we obtain two different stability ranges in the X and Y directions, also referred previously as YZ and XZ planes, respectively. This means that the cavity might be stable along one direction and unstable along the other. So, whenever we design FRL cavities, we shall look for the value of d (Actually, $d_x = d_y = d$ as it is the same geometrical parameter) that satisfies both inequalities (4) and (5). This was the main guideline for choosing the design parameters of our resonators. Table 1 below illustrates typical dimensions ranges, corresponding to different encountered situations: in the first case, stability is not reached at all, in the second case, we have stability along X axis and instability along Y axis, in the third case, we have instability along X axis and stability along Y axis. In the fourth case, we fulfill the stability conditions along both X and Y axis. From this last parameter range, we chose $d = 70.4 \mu\text{m}$ (and $R = 140 \mu\text{m}$) for our fabricated device.

Table 1. Stability conditions for different set of values for the geometrical cavity parameters R and d (n is fixed and equal to 1.47 and d_f is fixed and equal to $125 \mu\text{m}$)

R (μm)	d (μm)	Stable in X?	Stable in Y?
140] 133 , ∞ [No	No
140] 27.5 , 35 [Yes	No
140] 97.5 , 133 [No	Yes
140] 35 , 97.5 [Yes	Yes

EXPERIMENTAL RESULTS

The fabricated devices were tested using in-plane injection and detection by cleaved fibers. A tunable laser source is used in conjunction with a power-meter for achieving the wavelength sweep and recording the spectral response. The minimum recorded full width at half maximum (FWHM) is 0.1765 nm leading to a Q -factor of 8818. These values are obtained for a cavity having four silicon-air layers per mirror and a physical length $L = 265.8 \mu\text{m}$. Figure 4 shows the measured spectral response of this device. It is noteworthy, in our case, that the physical length is different from the optical length due to the presence of the FRL whose refractive index $n = 1.47$. Thus, the optical length is equal to $324.6 \mu\text{m}$.

Other devices with different number of Bragg layers were tested to study the impact of the mirror reflectance on the Q -factor. We find that as the number of layers increases, the Q -factor increases accordingly. These results confirm the trend of the Q -factor for an ideal FP cavity with planar mirrors given by:

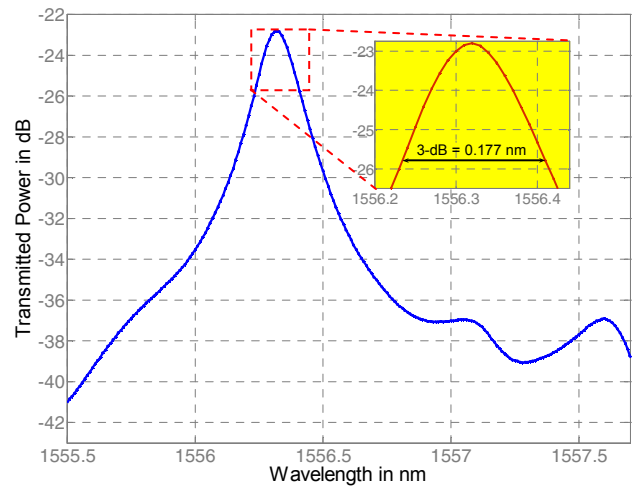


Figure 4: Measured Q -factor of 8818 on a cavity of length $L = 265.8 \mu\text{m}$, designed with cylindrical mirrors of radius of curvature $R = 140 \mu\text{m}$ with 4 silicon-air Bragg layers.

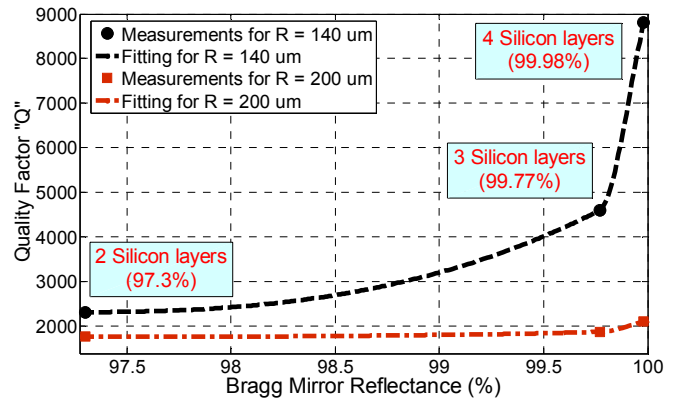


Figure 5: Measured Q -factor vs. reflectance of the curved Bragg mirrors for 2 cavities: The first has a length $L = 265.8 \mu\text{m}$ and radius of curvature $R = 140 \mu\text{m}$. The second has $L = 385.6 \mu\text{m}$ and $R = 200 \mu\text{m}$.

$$Q = \frac{2\pi nL}{\lambda_0} \left(\frac{\sqrt{\mathfrak{R}}}{1 - \mathfrak{R}} \right) \quad (6)$$

where L is the cavity length, n is the cavity refractive index, \mathfrak{R} the mirror reflectance, and λ_0 the free space wavelength. Figure 5 illustrates the relation between the number of Bragg layers (and hence the theoretically estimated mirror reflectance) with respect to the measured value of Q -factor for two cavities having different R . Cavity with smaller R was found to be more performant.

In order to mimic the tunability behavior of our resonators, spectral measurements have been carried out for cavities having similar design but differing only in their physical lengths. Two different cavity physical lengths ($L = 265.8$ and $280 \mu\text{m}$) have been measured, both are based on 4 silicon layers per mirror with a radius of curvature $R = 140 \mu\text{m}$. The measured spectral responses are shown in Figure 6. A simple test has been done to highlight the importance of

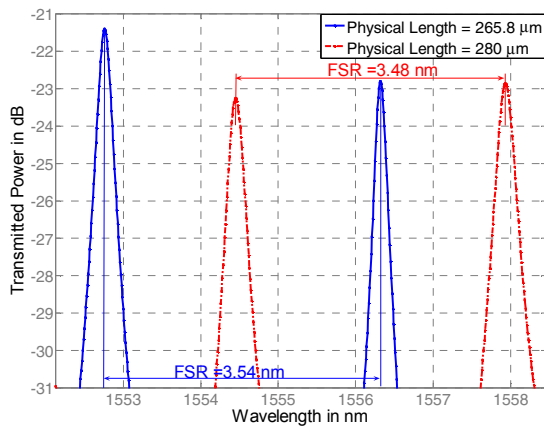


Figure 6: Measured spectral response of FRL cavities with two different cavity lengths $L = 265.8$ and $280 \mu\text{m}$. (The cylindrical mirrors have 4 silicon-air layers).

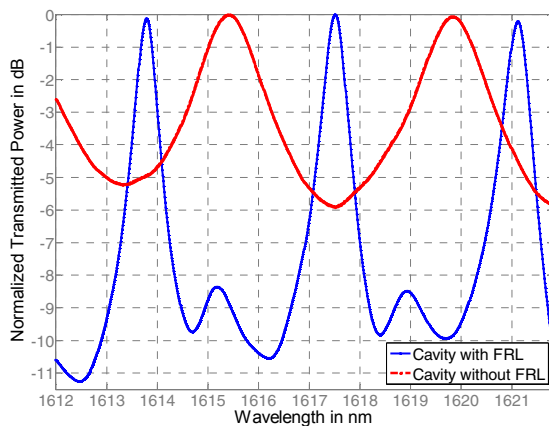


Figure 7: Comparison of measured responses with and without the FRL, illustrating the (3.68x) improvement in the Q -factor. (Here the mirrors consist of 2 silicon-air layers).

the FRL on the cavity performance. In this test, a design based on two silicon-air layers per mirror has been measured with and without insertion of the FRL. Though the reflectance of the two silicon-air layers is not very high, this device has been chosen for this specific illustration because it obeys the stability conditions in both cases with and without the FRL. Measurements show that the Q -factor improves by a factor of 3.68x for resonance wavelength around 1615 nm. The obtained results are shown in Figure 7. A similar improvement (4x) of the Q -factor has also been recorded for a cavity based on mirrors with 3 silicon layers.

CONCLUSION

In this work, we demonstrated a significant improvement to the Q -factor with respect to the conventional planar FP cavities operated in free-space with direct coupling to optical fibers. This improvement was obtained by introducing a new design including curved

Bragg mirrors together with Fiber Rod Lens, for the purpose of keeping the Gaussian beam focused after the multiple reflections inside the cavity, while keeping in the same time the benefit of high reflectance provided by using Bragg reflectors. Analytical modeling has been done to study the stability conditions for these new cavities, leading to the proper choice of dimensions set. Measurements show that a large Q -factor of 8818 was obtained for a cavity with 4 silicon-air layers. Tunability principle has also been demonstrated by measuring the spectral response of cavities having different physical lengths. It is believed that this novel FP cavity will open the way for numerous applications of high quality optical resonators working in free space.

ACKNOWLEDGEMENTS

The author thanks EGIDE and ESIEE-Paris for the grants offered to her to pursue her PhD project. Special thanks are due to the doctoral school MSTIC of Université Paris-Est for funding this part of the research project.

REFERENCES

- [1] B. Saadany, M. Malak, M. Kubota, F. Marty, Y. Mita, D. Khalil, and T. Bourouina, "Free-space Tunable and Drop Optical Filters Using Vertical Bragg Mirrors on Silicon", *IEEE J Sel Top Quant Electron.*, vol 12, no. 6, pp.1480-1488, 2006.
- [2] H. Cai, X. M. Zhang, A. B. Yu, Q. X. Zhang and A. Q. Liu, "MEMS tuning mechanism for eliminating mode hopping problem in external-cavity lasers", *IEEE MEMS conference*, pp. 159-162, 2007.
- [3] R. St.-Gelais, J. Masson, and Y.-A. Peter, "All-silicon integrated Fabry-Pérot cavity for volume refractive index measurement in microfluidic systems," *Appl. Phys. Lett.*, vol. 94, no. 24, pp.243905/1-243905/3, 2009.
- [4] S. Yun and J. Lee, "A Micromachined In-Plane Tunable Optical Filter Using the Thermo-optic Effect of Crystalline Silicon" *J. Micromech. Microeng.*, vol. 13, pp.721-725, 2003.
- [5] M.W. Pruessner, T.H. Stievater, and W.S. Rabinovich, "Reconfigurable Filters Using MEMS Resonators and Integrated Optical Microcavities", *IEEE MEMS conference*, pp.766-769, 2008.
- [6] A. Lipson and E. M. Yeatman, "A 1-D Photonic Band Gap Tunable Optical Filter in (110) Silicon" *J. Microelectromech. Syst.*, vol. 16, no.3, pp. 521-527, 2007.
- [7] A. Yariv, *Quantum Electronics*, John Wiley & Sons, 1989.
- [8] M. Malak, N. Pavy, F. Marty, E. Richalot, A.Q. Liu, T. Bourouina, "Design, Modeling and Characterization of Stable, High Q -factor Curved Fabry-Pérot cavities", accepted for publication in *J. Microsyst. Technol.*